

## MODELING AND OPTIMIZATION OF THIN-FILM SOLAR THERMOELECTRIC COOLING DEVICES

A. S. I. ABDALLA<sup>a</sup>, A. M. DAFALLA<sup>b</sup>, M. H. EISA<sup>c, d, \*</sup>, O. ALDAGHRI<sup>c</sup>,  
A. M. AL KAOUD<sup>c</sup>

<sup>a</sup> *Department of Physics, Faculty of Science, University of Kordofan, El-Obeid 10533, Sudan*

<sup>b</sup> *Laboratory of Advanced Energy Systems, CAS Key Laboratory of Renewable Energy, Guangzhou Institute of Energy Conversion, Chinese Academy of Sciences (CAS), China*

<sup>c</sup> *Department of Physics, College of Sciences, Imam Mohammad Ibn Saud Islamic University (IMSIU) Riyadh 11623, Saudi Arabia*

<sup>d</sup> *Physics Department, College of Science, Sudan University of Science Technology, Khartoum 11113, Sudan*

We present a mathematical model for a thin-film solar thermoelectric cooling and power generation depending on current flow at the interface between two different materials. Based on the direction of the current flow, an amount of thermal energy is absorbed or dissipated to offset the disparity in thermal energy between the two key materials. The reliability of thermoelectric energy transfer is obtained in terms of the power generation mode by applying two boundary clauses, one is the external heat input and the other is the temperature at the superior surface. Accordingly, to achieve an efficient and steady-state thermophotovoltaic process due to a thin-film solar cell system, a better understating of the solar energy conversion is needed. The calculated results owing to the process of solar cell conversion provide important intrinsic reliability for thin-film solar cells. with this approach, we address and analyze several modules composed of multiple n-type and p-type thermoelectric heterostructure that connected electrically in series and thermally in parallel.

(Received March 29, 2020; Accepted June 9, 2020)

*Keywords:* Modeling, Optimization, Thin-film solar, Thermoelectric devices, Cooling

### 1. Introduction

The temperature difference between optoelectronic and microelectronic components is generally achieved with thermoelectric (TE) cooler to obtain a better performance [1]. Therefore, TE cooler is considered as a modern nanotechnology and optical telecommunication that contributes to stability characteristics of optical sources and routine or swap components that used in sunlight systems. Moreover, the resultant temperature gradient in thermoelectric thin-film (TETF) devices is widely used to generate electricity via the function between the two dissimilar conductors [2]. Recently, the importance of cooling in microprocessors and other integrated circuits is significantly increased due to the growth in clock speed and the reduction of distinguished size. The devices become micro-size, faster, and denser, when the heat power density has vastly risen [3].

The technology of bulk fabrication and packaged modules of the thermoelectric cooler are reliable and usually limited. That makes the complementarily of optoelectronic and microelectronic devices more difficult, and increases the cost of packaging. Consequently, to avoid such as problems, the shift from bulk thermo-elements to integrated thin-film thermoelectric cooler is significant [3-5]. TETF coolers are mainly applied to increase the gain in cooling power density along to the thermo-elements device. Besides, many techniques deal with this trouble are studied

---

\* Corresponding author: mheisas@hotmail.com

to improve the functioning of bulk thermo-elements, such as the reduced thermal conductivity in thin-films [9-11] and the resurgence emission in heterostructures [3,6].

In addition, thin-film coolers can be employed in large quantities using integrated circuit cluster fabrication techniques, which results in lowering the costs and increasing the efficiency. It is feasible for efficient localized cooling, to integrate between the devices of the microelectronic and the optoelectronic [5]. When transferred from bulk to TETF coolers, the non-ideal factors become clearly and must consider. While contact resistance, thermal resistance of the heat cesspool, and current flows due to heat power are secondary impacts in bulk TE coolers, these all become critical in TETF coolers.

Recent theoretical analysis of the TETF coolers relying on many materials [12-16], indicating that the operating temperature is one of the key parameters for the thin-film coolers. However, their connection with the TETF solar devices is not yet quantified for which the commonly adopted approach is to take the temperature a model parameter [16-18]. Therefore, considering and investigating the different materials under various operating and design parameters is important in order to optimize their performance. Hence, more detailed theoretical studies on several coefficients that limit the thin-film coolers performance and power generation are needed. The present work is organized as follows. In Sec. II, we introduce the mathematical modeling for the TE cooling devices. In Sec. III, we addressed the simulation methods and boundary conditions of the specific problem. Numerical results and discussion are shown in Sec. IV which is separated into two subsections according to simulation model. Finally, a brief conclusion is summarized in Sec. V.

## 2. Modeling of the devices

### 2.1. Mathematical formula

The Peltier effect examines the dissipation or absorption of heat at a junction among two various contactors when a current flow through an interface of two different types of substances with temperature deference on each side [5]. Based on the direction of current flow, a thermal energy is absorbed or dissipated in order to offset the disparity in thermal energy that transported in the two materials. The rate  $dQ/dt$  of heat created or absorbed at embeds between contactors A and B [7] is expressed as:

$$dQ/dt = (\Pi_A - \Pi_B) I \quad (1)$$

where,  $\Pi_A$  and  $\Pi_B$  are Peltier's coefficients of the conductors, and the parameter  $I$  is the electric current. The two different conductor's junction with production of electromotive force (EMF) is called the Seebeck Effect [7,8]. Two junctions connected back to maintain at two different temperatures  $T_1$  and  $T_2$  and an EMF voltage appears between their free contacts:

$$V = -S(T_1 - T_2) \quad (2)$$

where  $S$  is Seebeck's coefficient. The Thomson effect is the production or absorption of heat along a contactor with temperature gradient  $\Delta T$  when electric charge flows through it. An amount of heat  $dq/dt$  is produced or absorbed along the conductor segment is:

$$dq/dt = -KJ\Delta T \quad (3)$$

where  $K$  is Thomson's coefficient and  $J$  is the current density. The relationship between the abovementioned coefficients are linked through Kelvin relations, which can be expressed as:

$$\Pi = TS \quad (4)$$

where,  $\Pi = \Pi_A - \Pi_B$  and  $K = T dS/dT$ .

In this work, we proposed that the value of thermal energy  $Q$  is transported by a current  $I$  in a material having a Seebeck coefficient  $S$  at absolute temperature  $T$ , is given by  $Q = STI$ . Thus, the absorbed or dissipated heat at the interface between material 1 and material 2 by the Peltier effect becomes equal to the difference of the transported thermal energies or:

$$Q_1 - Q_2 = S_1 - S_2 TI. \quad (5)$$

Moreover, there are other thermal transport effects such as Joule heating and thermal condition. The Joule heating in a material with electrical resistance  $R$  is identified as  $I^2 R$ . This amount of heat is equally divided and propagated to the two ends of the material. When a temperature gradient is created through a material, the heat conduction occurs from the hot side to cold side, and it is ought to be proportional to the temperature gradient  $\Delta T$ , so that  $Q_{\text{cond}} = \Delta T/R_T$ , where  $R_T$  is the thermal resistance of the material.

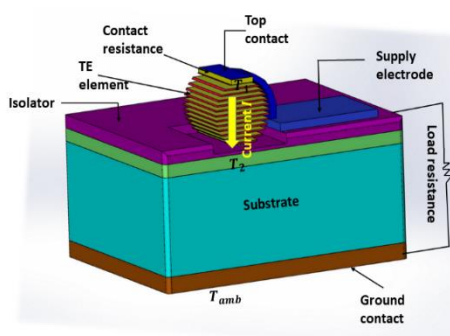


Fig. 1. Schematic of a thin-film TE device fabricated on a conducting substrate.

Fig. 1 shows a typical structure of a TETF device processed on a conducting substrate. A top metal contact is filed on the upper side of the TETF component, and the lower contact is filed at the bottom of the substrate, therefore, when the system works, the TFTE is designed to allow the electrical current loading and the heat flow vertically cross the entire structure. In our approach, we solve the heat balance equations by considering both the generated heat at the upper surface of the TE element and at the surface heat transport between the TE components [9]. For example, at the top surface, the heat equilibrium equation contains a detailed account of heat generation terms due to Peltier heat, Joule heat, and heat contactor, which is formulated as:

$$Q_1 + \frac{1}{2} R_E I^2 + R_C I^2 - S_{TE} T_1 I - \frac{(T_1 - T_2)}{R_T} = 0. \quad (6)$$

where  $Q_1$  is the external heat input,  $R_E$  is the electrical resistance of the TE element,  $R_C$  is the contact resistance at the interface of the top contact metal and the TE element,  $S_{TE}$  is the Seebeck coefficient of the TE element,  $T_1$  is the temperature at the top surface,  $T_2$  is the temperature at the interface between the TE component and the substrate,  $R_T$  is thermal resistance of the TE element. For simplicity, we assume an ideal metal contact, which has negligibly small thermal resistance and Seebeck coefficient. On the other hand, at the interface of the TE component and the substrate, the second heat equilibrium equation is constructed as:

$$\frac{1}{2} R_E I^2 + \frac{1}{2} R_{\text{sub}} I^2 - (S_{\text{sub}} - S_{TE}) T_2 I + \frac{(T_1 - T_2)}{R_T} - \frac{(T_2 - T_{\text{sub}})}{R_{\text{sub}}} = 0 \quad (7)$$

where  $R_{\text{sub}}$  is the electrical resistance of the substrate that includes electrical spreading effect,  $S_{\text{sub}}$  is the Seebeck coefficient of the substrate,  $R_{\text{sub}}$  is the thermal resistance of the substrate that includes thermophotovoltaic in the substrate [5]. We considered that the bottom contact to be

connected to an ideal heat sink, so that its temperature stays fixed at ambient temperature  $T_{amb}$  during the operation.

A locked model thermal deployed resistance in a substrate is relied from Lee et al. [4] with hypothesis of an infinitely significant substrate and an ideal heat sink under it. Compared the electrical deployed resistance is earned from Vashaee et al. [2], which is based on ANSYS finite element simulation.

### 3. Simulation method and boundary conditions

We proposed an equivalent circuit mode that very much similar to the one used for modelling of InP thin-film coolers by Vashaee et al. [5]. However, since the side metal contact is strongly affecting the performance of the cooler, we use a more realistic model for Joule heating in the side contact, and heat contactor from the cold embeds to substrate through this contact. Thermoelectric devices work as both a cooler and a power generator. The detailed simulation and modeling of side contact will allow us to optimize its geometry [17].

#### 3.1. Cooling model

In the cooling model, a current is pumped into the TE device. Two limits terms can be simulated: one is that the cooling power  $Q_1$  is known, from which  $T_1$  and  $T_2$  are computed by solving the paired heat equilibrium equations (6) and (7) [1]. The other limit term is that the upper side temperature  $T_1$  is known, from which  $T_2$  and the cooling power  $Q_1$  are computed [17, 18]. Then the coefficient of performance (COP), is obtained by

$$COP = Q_1/W \quad (8)$$

where  $W$  is refer to the work done by the electrical current to do the cooling performance, which is given as

$$W = IV_{oc} + I^2R_i \quad (9)$$

where  $V_{oc}$  is the open-circuit voltage that internally caused within the device by the Seebeck effect,  $V_{oc} = S_{TE}(T_1 - T_2) + S_{sub}(T_2 - T_{sub})$ , and  $R_i$  is the total internal resistance of the device,  $R_i = R_C + R_T + R_{sub}$  [17]. The first term on the right hand side of Eq. (9) describes the work done against the open-circuit voltage that induced internally in the device by the Seebeck effect, and the second term describes the electrical power consumed in the entire device [7].

#### 3.2. Power generation model

In the power generation model, heat energy  $Q_1$  is pumped to the device at the top that create a gradient of temperature through the device, and also generate a voltage by the Seebeck effect. When a load resistance  $R_L$  is connected to the device, the current flow through the system and creates the power output,  $P_{out} = I^2R_L$  [7]. The current is obtained because an electrical circuit model with an internal resistance  $R_i$  is connected to an external load  $R_L$ , as the following expression [5]:

$$I = \frac{V_{oc}}{R_i + R_L} \quad (10)$$

We also apply two limits terms to simulate the power generation model. One is that the heat input  $Q_1$  is known, and then we calculate  $T_1, T_2$ , and  $I$  by solving the coupled heat balance equations (6) and (7) and using Eq. (10). The other limit is that  $T_1$  is known, and we calculate  $Q_1, T_2$  and  $I$  by the same procedure. Then the TE energy conversion efficiency  $\eta$  is achieved by

$$\eta = P_{out}/Q_1 \quad (11)$$

In this study, we simulate the TE module with substrate and without substrate, considering both the cooling and power generation modes. Then the simulation results are compared using online simulator tools as presented in Ref. [17]. In addition, we analyze the TE figure of feature reliability and voltage as the function of load resistance and we verified that the greatest values of thin-film originate from a reduction resistance load in the thermal conductivity. We started by fabricate new geometry Fig. 1 where the top contact can be adapted to optimize the mechanism of cooling, therefore, one can optimize the width of the top contact layer, assuming a fixed length and fixed thin film thickness.

## 4. Results and discussion

### 4.1. Results and discussion of cooling model

In this mode, we set the cooling power density to be  $Q_{in}=100$  W, the model solves for temperatures ( $T_1$ ,  $T_2$ ) with a given applied current  $I = 0.5$  A, the total electric power consumed ( W) and the coefficient of performance in Eq. (8) are obtained as function of the thin film thickness in micrometers. In Figs. (2) and (3), both the electric current and heat spreading effects of the substrate are taken into account. Throughout this mode we adopted the substrate properties as: the Seebeck coefficient is ( $-50 \mu\text{V/K}$ ), the thermal conductivity is  $100$  W/mK, the electrical conductivity is  $10000 \Omega^{-1} \cdot \text{cm}^{-1}$ , and the thickness of substrate is  $500 \mu\text{m}$ .

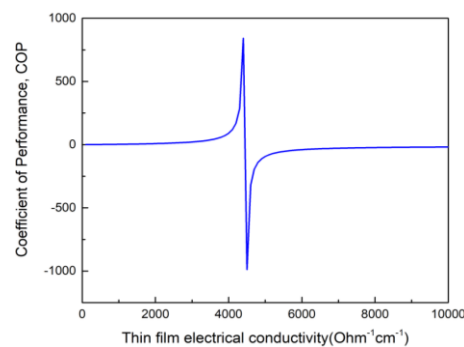


Fig. 2. Show the coefficient of performance as function of a thin-film electrical conductivity.

Thin-film properties have also adopted via this mode as follow: the Seebeck coefficient is ( $-200 \mu\text{V/K}$ ), thermal and electrical conductivity of thin-film are  $1$  W/mK, and  $1000$  W/mK, respectively, the thickness is  $20 \mu\text{m}$ , and the selected contact resistance is  $10^{-7} \Omega \text{ cm}^2$ .

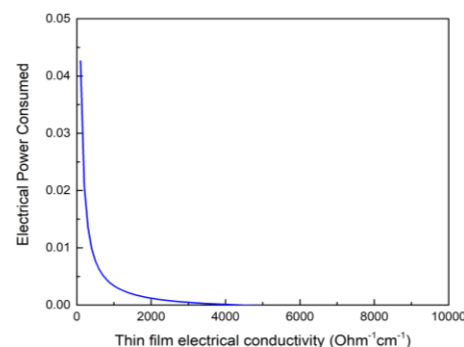


Fig. 3. Show the electrical power consumed as function of a thin-film electrical conductivity.

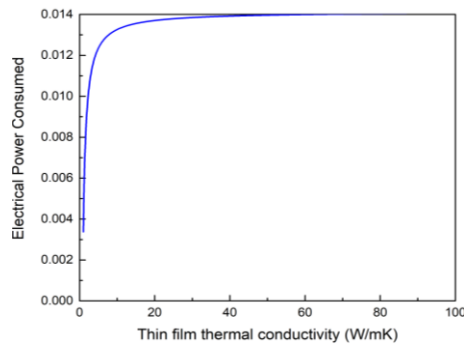


Fig. 4. Show the electrical power consumed as function of a thin-film thermal conductivity.

The geometry of the TETF has device was described in Fig. 1. Figs. 2 and 3 show the coefficient of performance and the consumed electrical power as function of the thin-film thermal conductivity, respectively. On the other hand, the effect of the thin film thermal conductivity on the consumed electrical power is presented in Fig.4. Based on the p-type Si-substrate, we found that the COP and the consumed electrical power are considerably influenced by the electrical and thermal conductivity of the thin-film, and their values consequently deposition over operation. There are several studies on the thermoelectric cooling Models where he presented each of Abdullah et al. [19] have carried out an experimental study on cooling performance of a developed hybrid Solar Thermoelectric- Adsorption cooling system.

#### 4.2. Results and discussion of power generation model:

In this subsection, we simulated TETF power generator as function of load resistance where the heat power density ( $Q_{in}$ ) that imposed in the TE layer from top is known. In the substrate, both electrical current and heat spreading effects are examined. A load resistance  $R_L$  is associated with the device, therefore a current flow crosses the load to create a power outcome,  $P_{out} = I^2 R_L$  and the power generation efficiency as given by Eq. (11) is also obtained.

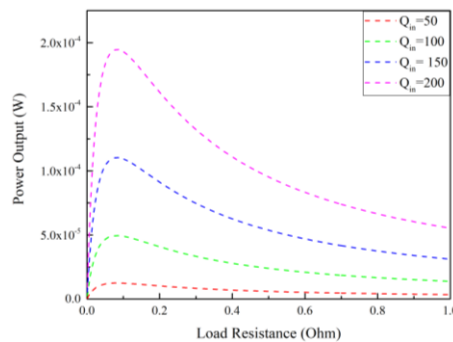


Fig. 5. Show the power output as function of load resistance at various heat power density  $Q_{in}$ .

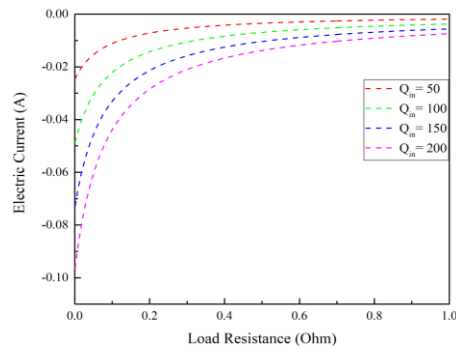


Fig. 6. Show the power output as function of load resistance at various heat power density  $Q_{in}$ .

Figs. 5-8 illustrate the measured power output, efficiency, and voltage under different device load resistance using power generator model. Our calculation depending on this model allows us to determine the power efficiency from the initial heat power density  $Q_{in} = 50, 100, 150,$  and  $200$  W, and clearly we can observe that the power output and reliability current trend decreases as we increased the load resistance, i.e. the smaller load resistance are more effective. Figs. 6 and 8 demonstrate that the electric current and voltage across the load, one can see that head load from TE devices increases the electric current and voltages through the load increment.

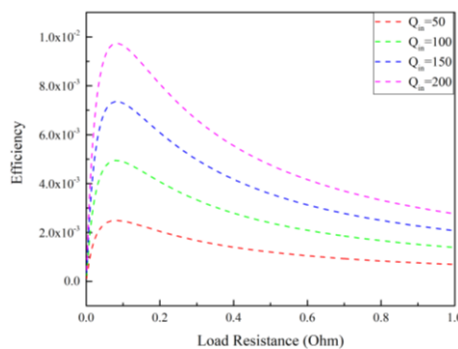


Fig. 7. Show the power generator efficiency as function of load resistance at various heat power density  $Q_{in}$ .

It is shown that the thermoelectric can impact the TF heterostructures thermoelectric device. In addition, we have considered the influence of thermoelectric temperature on micro coolers, and we also considered the implications of ohmic conductor and substrate resistances.

The geometry of the top contact can be adapted to optimize the mechanism of cooling. To achieve that, two effects need to be considered: joule heating in the top contact layer and heat contact from substrate to the cold junction (see Fig. 1). When the top contact is very tight, the heat conduction will be minimized, but there will be a significant joule heating. In contrast, if the top contact is very broad or metal contact, the joule heat will be decreased, and that may promote the amount of generated heat due conduction. Therefore, one can optimize the width of the top contact layer, assuming a fixed length and fixed thin film thickness.

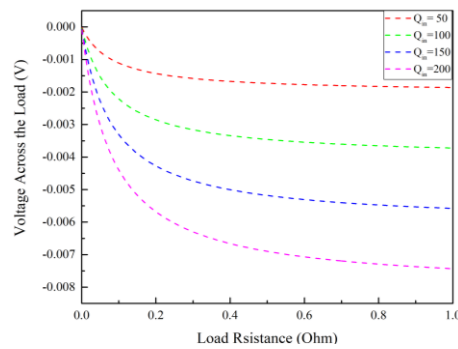


Fig. 8. Show the voltage across the load resistance at different heat power density  $Q_{in}$ .

## 5. Conclusions

In this paper, we numerically investigate the thermoelectric cooling and power generation density modes in a thin film heterostructure thermoelectric device. Practically, thermoelectric modular composed of several p-type and n-type components that are connected electrically in series, and thermally in parallel are considered. Based on thin-film TE device parameters and boundary conditions, the geometry has been proposed and investigated with several micro-coolers. The coefficient of performance and TE energy conversion reliability are presented. Furthermore, an optimized geometry for the side contact is proposed to increase the electricity and promote the heat during concentration of solar cells energy. The results predictions show that increasing the heat power density input of the thin-film TE device results in decreasing their performance and degrading their efficiency. It is shown that the thermoelectric can impact the TF heterostructure thermoelectric device and can be utilized in future work to examine the intrinsic capability of thin film solar cells.

## Acknowledgments

The authors would like to thank friends for generous support, valuable discussions and comments.

## References

- [1] L. Rushing, A. Shakouri, P. Abraham, J. E. Bowers, Germany, Proc. of 16th Int. Conf. on Thermoelectrics, Dresden, 646, 1997.
- [2] T. A. Corser, Atlanta, GA, 41st Electronic Components and Technology Conference, 150, 1991.
- [3] D. Vashaee, J. Christofferson, Y. Zhang, A. Shakouri, G. Zeng, C. LaBounty, X. Fan, J. Piprek, J. E. Bowers, E. Croke, Micro. Thermophysical Eng. **9**, 99 (2005).
- [4] S. Lee, S. Song, V. Au, K. P. Moran, Proc. of the 4th ASME/JSME Thermal Eng. Joint Conf. **4**, 199 (1995).
- [5] D. Vashaee, J. Christofferson, Y. Zhang, A. Shakouri, G. Zeng, C. LaBounty, X. Fan, C. LaBounty, J. Piprek, J. E. Bowers, E. Croke, Mic. Thermophysical Eng. **9**, 99 (2005).
- [6] A. Shakouri, C. LaBounty, J. Piprek, P. Abraham, J. E. Bowers, Appl. Phys. Lett. **74**, 88 (1999).
- [7] D. K. C. MacDonald, 2006, (New York: Dover Publications–Interscience).
- [8] S. Dongaonkar, J. D. Servaites, G. M. Ford, S. Loser, J. Moore, R. M. Gelfand, H. Mosheni, H. W. Hillouse, R. Agrawal, M. A. Ratner, T. J. Marks, M. S. Lundstrom, M. A. Alam, J. Appl. Phys. **108**, 124509 (2010).
- [9] P. Hyldgaard, G. D. Mahan, Phys. Rev. B **56**, 10754 (1997).

- [10] G. Chen, Phys. Rev. B **57**, 14958 (1998).
- [11] G. Chen, 1998, Nat. **413**(6856), 597 (1998).
- [12] R. Venkatasubramanian, E. Siivola, T. Colpitts, B. O'Quinn, K. Coonley, P. Addepalli, J. Posthill, M. Puchan, Long Beach, CA, Proc. of the 21st Int. Conf. on Thermoelectrics, 528, 2002.
- [13] B. Yang, J. L. Liu, K. L. Wang, G. Chen, Mat. Res. Soc. Symp. Proc. **691**, 71 (2001).
- [14] C. LaBounty, A. Shakouri, J. E. Broers, J. Appl. Phys. **89**(7), 4059 (2001).
- [15] X. Fan, G. Zeng, C. LaBounty, E. Croke, D. Vashae, A. Shakouri, C. Ahn, J. E. Bowers, Elec. Lett. **37**(2), 126 (2001).
- [16] Martin A Green, Stephen P. Bremner, Nat. Mat. **17**, 23 (2016).
- [17] J.-H. Bahk, M. Youngs, K. Yazawa, O. Pantchenko, A. Shakouri, 2014, <https://nanohub.org/resources/thermo>.
- [18] A. Bulusu, D. G. Walker, J. Appl. Phys. **102**, 073713 (2007).
- [19] M. O. Abdullah, J. L. Ngui, K. Abd.Hamid, S. L. Leo, Ener. Fuels **23**, 5677.